ELSEVIER

Contents lists available at ScienceDirect

Colloids and Surfaces A: Physicochemical and Engineering Aspects

journal homepage: www.elsevier.com/locate/colsurfa





Synthesis and characterization of carbon dots derived from compounds containing thioureas and thiazole rings

Suhair M.S. Jambi ^{a,1}, Jiuyan Chen ^{b,1}, Wei Zhang ^b, Shiwei Fu ^b, Yiqun Zhou ^b, Justin B. Domena ^b, Nicholas Michael Brejcha ^c, Fuwu Zhang ^b, Roger M. Leblanc ^{b,*}

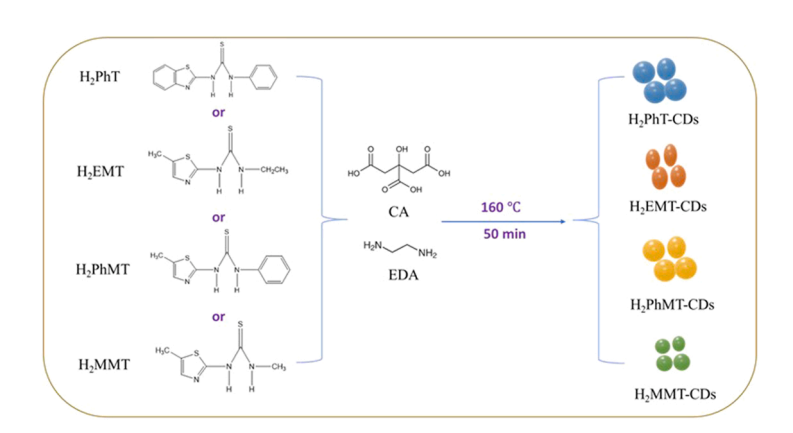
- a Department of Chemistry, University of Jeddah, Jeddah, Saudi Arabia
- ^b Department of Chemistry, University of Miami, Coral Gables, FL 33146, USA
- ^c Department of Biochemistry and Molecular Biology, Miller School of Medicine, University of Miami, Coral Gables, FL 33146, USA

HIGHLIGHTS

Four kinds of CDs derived from molecules that contain thioureas and thiazole rings were firstly prepared.

- The structural properties of these CDs were conducted to prove the residual structures of therapeutical compounds.
- These four families of CDs have potential in the treatment of diabetes, cancer, and infections in future research.

GRAPHICAL ABSTRACT



ARTICLE INFO

Keywords:
Carbon dots
Thioureas
Thiazole
Characterization
Potential therapeutic treatment

ABSTRACT

Synthesizing carbon dots (CDs) using therapeutic compounds as precursors is a new trend in the applications of CDs in drug delivery and disease treatment by leveraging the advantages of nanoparticles and therapeutic molecules simultaneously, without the need of further modifications. Compounds containing thioureas and thiazole rings have been extensively studied in biological applications such as antidiabetic, anticancer, antimicrobial, antiviral and antifungal activities. However, the research using such compounds as precursors to synthesize CDs has not been reported. In this study, four types of CDs derived from 1-(benzo[d]thiazol-2-yl) – 3-phenylthiourea (H₂PhT), N-ethyl-N'-(4'-methylthiazol-2'-yl) thiourea (H₂EMT), N-phenyl-N'-(4'-methylthiazol-2'-yl)thiourea (H₂PhMT) or N-methyl-N'-(4'-methylthiazol-2'-yl)thiourea (H₂MMT) were successfully prepared and characterized. The UV-vis absorption, fluorescence, and Fourier-transform infrared (FTIR) spectroscopies, atomic force microscopy (AFM), zeta potential measurements and thermogravimetric analysis (TGA) suggested that these four families of CDs are all less than 10 nm. H₂PhT-CDs, H₂EMT-CDs, and H₂PhMT-CDs possess excitation-independent PL emission at around 440 nm, while H₂MMT-CDs exhibit excitation-dependent PL

E-mail address: rml@miami.edu (R.M. Leblanc).

^{*} Corresponding author.

¹ Both authors contribute equally to this work

emission property. The structural properties of CDs indicate the presence of certain moieties that may be associated with the therapeutic effects of H_2PhT , H_2EMT , H_2PhMT and H_2MMT in the corresponding H_2PhT -CDs, H_2EMT -CDs, H_2PhMT -CDs and H_2MMT -CDs. Moreover, all four families of CDs possess a slightly positive or negative charge, which benefits their affinities to cells. The results in this study could provide the knowledge in understanding the potential applications of these CDs in the treatment of diabetes, cancer, and infections in future research.

1. Introduction

Owing to the properties of overcoming the disadvantages of conventional drugs by adjusting pharmacokinetics and delivery, which can diminish side effects and improve efficiency, nanomaterials have attracted great attention in medical applications. [1] Among the various type of nanomaterials, carbon dots (CDs), emerging carbon-based nanoparticles that possess a small size less than 10 nm, excellent optical properties, good water solubility, prominent biocompatibility, and tunable functionalized surface, have been widely applied in the fields of photocatalysis, bioimaging, biosensing, drug delivery, gene therapy, photothermal therapy, and tissue engineering. [2–5] Regarding disease treatment, conjugation of CDs with drugs is a commonly used approach to enhance treatment efficiency and improve targeting abilities.

Recently, several drug-derived CDs prepared by using compounds with anticancer, antivirals and antibacterial capabilities have been reported. These CDs showed advantages in selective targeting, enhanced treatment efficiency and lower drug resistance compared to pure drugs. [6–9] For example, Lu et al. developed gallic acid-based CDs (GACDs) and investigated their antitumor activities in vitro and in vivo. The results displayed that GACDs-treated mice showed significantly reduced tumor growth. Moreover, GACDs had a more dramatic antitumor effect than pure GA. [8] In our previous work, we prepared a cationic CD species (Y15-CDs) using 1, 2, 4, 5-benzenetetramine (Y15, a focal adhesion kinase inhibitor), folic acid and ethylenediamine as precursors to explore the impact of drug-derived CDs on growth of cancer and normal cells. The bioimaging and cytotoxicity studies demonstrated that Y15-CDs could target the cellular nucleus and exhibit a higher cytotoxicity to cancer cells than to normal cells. [6] Different from utilizing anticancer drugs, Wu et al. applied Levofloxacin, one of quinolones with strong antibacterial effect, as single precursor to synthesize CDs. The obtained CDs had excellent antibacterial activity and biocompatibility in vitro and in vivo. [7] Huang et al. prepared a type of benzoxazine monomer derived CDs (BZM-CDs) for antiviral therapies. It was proved that BZM-CDs were active against both flaviviruses and non-enveloped viruses in vitro. [9] Thus, synthesis of CDs via using therapeutic compounds as precursors become new tendency in application of CDs in medical fields.

Thioureas containing thiazole rings have been found to possess a wide range of biological applications including antidiabetic, anticancer, antimicrobial, antiviral and antifungal properties. In this study, four kinds of CDs derived from molecules that contain thioureas and thiazole rings including 1-(benzo[d]thiazol-2-yl) - 3-phenylthiourea (H₂PhT), Nethyl-N'-(4'-methylthiazol-2'-yl) thiourea (H2EMT), N-phenyl-N'-(4'methylthiazol-2'-yl)thiourea (H₂PhMT) and N-methyl-N'-(4'-methylthiazol-2'-yl)thiourea (H2MMT) were prepared, respectively, via a solvothermal approach. Then, the acquired H₂PhT-CDs, H₂EMT-CDs, H₂PhMT-CDs, and H₂MMT-CDs were characterized through UV-vis absorption, fluorescence, and Fourier-transform infrared (FTIR) spectroscopies, atomic force microscopy (AFM), zeta potential measurements and thermogravimetric analysis (TGA). As the physiochemical and structure properties of CDs are highly related to the therapeutic efficiency, the outcomes of this research have the potential to serve as a basis for forthcoming studies which will focus on the therapeutic efficacy of these CDs in the treatment of diabetes, cancer, and microbial infections.

2. Experimental sections

2.1. Materials and reagents

Citric acid (CA), 2-aminobenzothiazole, 2-amino-4-methylthiazole, ethyl isothiocyanate, phenyl isothiocyanate and methyl isothiocyanate were bought from Sigma-Aldrich (St Louis, MO, USA). 1,2-ethylenediamine (EDA, \geq 99%) was purchased from Thermo Scientific (Waltham, MA, USA). The deionized (DI) water was purified by a Modulab 2020 water purification system bought from Continental Water System Corporation. (San Antonio, TX, USA). The resistivity and surface tension of DI water were set at 18.2 M Ω .cm and 72.6 mN·m $^{-1}$, respectively, at 22 °C. All reagents were used without further modification.

2.2. Instrumentations

Nuclear magnetic resonance (NMR) spectra were acquired on an Advance NEO 500 MHz spectrometer (Bruker, USA). Mass spectra were obtained on a MicroQ-TOF ESI mass spectrometer (Bruker, USA). The UV-vis absorption and fluorescence emission spectra were recorded by using a Cary 100 UV/vis spectrophotometer (Agilent Technologies, USA) and a Fluorolog-3 fluorometer (Horiba Jobin Yvon, USA) and, respectively. The quartz cells used for UV-vis and fluorescence emission spectra detection are both with a pathlength of 1 cm. FTIR spectra were measured by a PerkinElmer Fourier-transform infrared spectrometer (Frontier, PerkinElmer, USA) equipped with Smart Orbit attenuated total reflectance accessories (Thermo Scientific, USA). The morphologies of CDs were observed via a 5420 at. force microscope (AFM) (Agilent Technologies, USA) by using the taping mode. The zeta potential measurement was performed on a nano series Malvern Zetasizer (Malvern Panalytical, USA). TGA was measured via a TG 209 F3 Tarsus thermo-microbalance (Netzsch, USA) with the heating temperature ranged from 40 to 1000 °C at a rate of 10 °C/min under the protection of nitrogen. The flowrate of nitrogen was 10 mL/min.

2.3. Synthesis of 1-(benzo[d]thiazol-2-yl)- 3-phenylthiourea (H_2PhT)

H₂PhT was prepared with the published method. [10] 2-aminobenzothiazole (0.01 mol) was mixed with phenyl isothiocyanate (0.01 mol) in 30 mL hot ethanol and stirred for 3.5 h. After cooling down to room temperature, the precipitate was filtered off, washed with ethanol, and recrystallized from ethanol. The obtained compound was confirmed by 1 H NMR and mass spectroscopy measurements. 1 H NMR spectra are shown in Fig. S1: 1 H NMR (500 MHz, DMSO- d_6) δ 13.16 (s, 1 H), 10.41 (s, 1 H), 7.85 (d, J=7.7 Hz, 1 H), 7.70 (d, J=7.9 Hz, 2 H), 7.60–7.45 (m, 1 H), 7.45–7.40 (m, 1 H), 7.35 (t, J=7.8 Hz, 2 H), 7.31–7.25 (m, 1 H), 7.14 (s, 1 H). The calculated molecular weight: 285.3830. Found in mass spectra (Fig. S2A): 308.0289 (M+Na) $^+$. Fig. 1 shows the chemical structure of H₂PhT.

2.4. Synthesis of N-ethyl-N'-(4'-methylthiazol-2'-yl) thiourea (H_2EMT), N-phenyl-N'-(4'-methylthiazol-2'-yl)thiourea (H_2PhMT) and N-methyl-N'-(4'-methylthiazol-2'-yl)thiourea (H_2MMT)

 H_2EMT , H_2PhMT and H_2MMT were synthesized according to the published literature. [11] 0.01 mol of 2-amino-4-methylthiazole was dissolved in 20 mL of ethanol and stirred. Then 0.01 mol of ethyl

Fig. 1. Chemical structures of compound $\rm H_2PhT$, $\rm H_2EMT$, $\rm H_2PhMT$ and $\rm H_2MMT$.

isothiocyanate, phenyl isothiocyanate or methyl isothiocyanate was added to the solution and refluxed for 3 days. The precipitates were separated and recrystallized by hot ethanol. The ^1H NMR and mass spectral measurements of obtained H₂EMT, H₂PhMT and H₂MMT are shown in Fig. S1 and Fig. S2, respectively. For H₂EMT: ^1H NMR (500 MHz, DMSO- d_6) δ 11.46 (s, 1 H), 9.62 (s, 1 H), 6.62 (s, 1 H), 3.53 (dt, J=12.5, 6.2 Hz, 2 H), 2.22 (s, 3 H), 1.16 (t, J=7.2 Hz, 3 H). The calculated molecular weight: 201.3060. Found: 224.0285 (M+Na)⁺ (Fig. S2B). For H₂PhMT: ^1H NMR (500 MHz, DMSO- d_6) δ 12.48 (s, 1 H),

10.15 (s, 1 H), 7.71 (d, J = 7.9 Hz, 2 H), 7.30 (t, J = 7.8 Hz, 2 H), 7.06 (t, J = 7.4 Hz, 1 H), 6.54 (s, 1 H), 2.23 (d, J = 1.2 Hz, 3 H). The calculated molecular weight: 249.3500. Found: 250.0465 (M) $^+$ (Fig. S2C). For H₂MMT: 1 H NMR (500 MHz, DMSO- d_6) δ 11.56 (s, 1 H), 9.55 (s, 1 H), 6.61 (s, 1 H), 3.01 (d, J = 4.6 Hz, 3 H), 2.22 (s, 3 H). The calculated molecular weight: 187.2790. Found: 210.0129 (M+Na) $^+$ (Fig. S2D). The structures of H₂EMT, H₂PhMT and H₂MMT are shown in Fig. 1.

2.5. Synthesis of H_2PhT -CDs, H_2EMT -CDs, H_2PhMT -CDs and H_2MMT -CDs

Four families of CDs were prepared via a solvothermal approach. Briefly, for H_2PhT -CDs, nitrogen gas was used to drive air from round-bottomed flask for 5 min. Then 10 mL of EDA was added to the round-bottomed flask and heated in an oil bath. When the temperature reached 160 °C, 2.0 g of citric acid and 0.1 g of H_2PhT were added by vigorously stirring. After refluxing and reacting for 50 min, the solution was cooled down to room temperature and rinsed with acetone more than 3 times. Finally, the obtained CDs were dispersed in 20 mL of DI water and heated by a rotary evaporator to completely evaporate water and acetone. H_2EMT -CDs, H_2PhMT -CDs and H_2MMT -CDs were prepared via the same approach as H_2PhT -CDs by changing H_2PhT to H_2EMT -CDs, H_2PhMT -CDs, respectively.

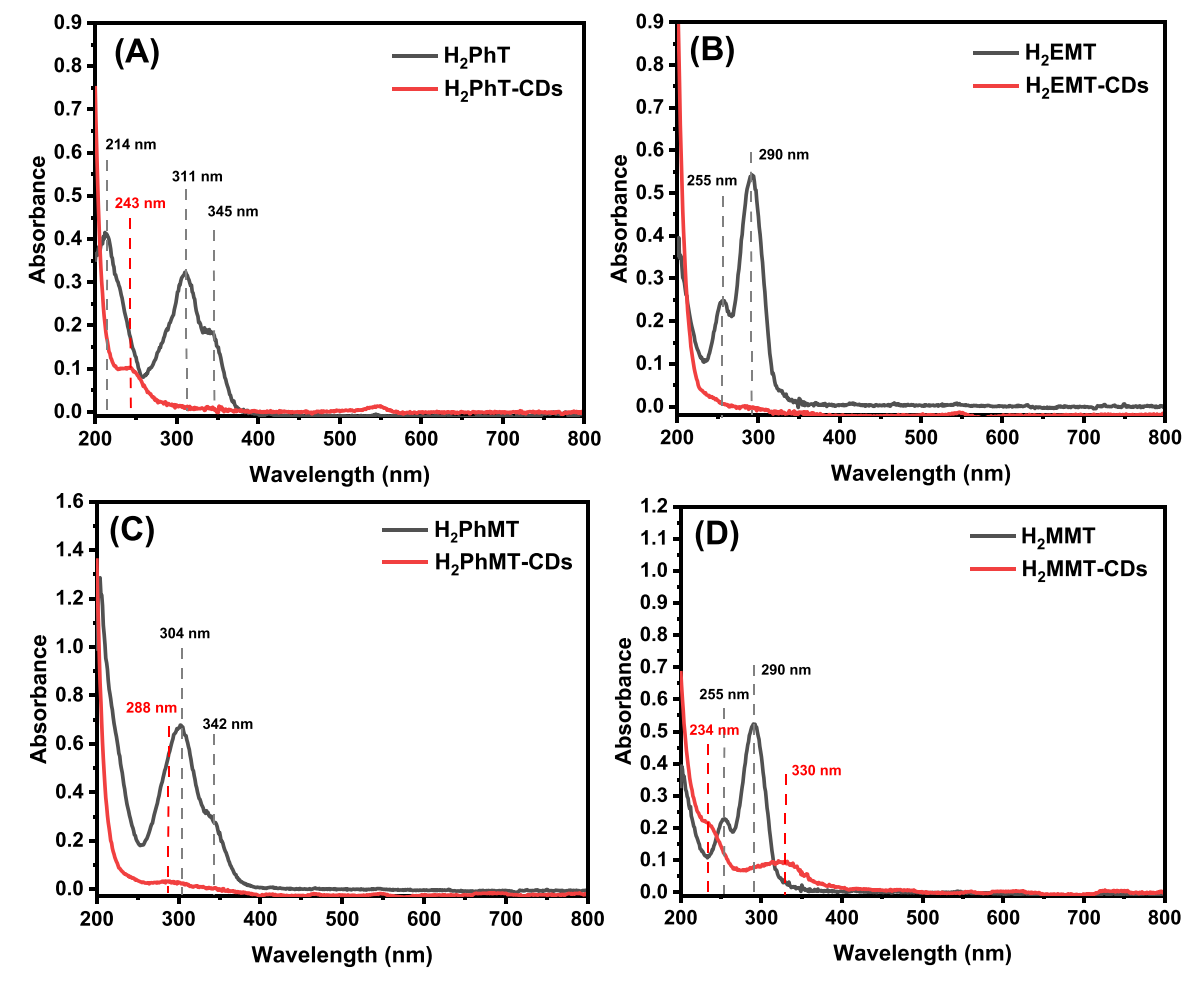


Fig. 2. UV-vis spectra of (A) H₂PhT and H₂PhT-CDs; (B) H₂EMT and H₂EMT-CDs; (C) H₂PhMT and H₂PhMT-CDs; and (D) H₂MMT and H₂MMT-CDs.

3. Results and discussion

3.1. UV-vis spectra

The absorption spectra of H₂PhT, H₂EMT, H₂PhMT, H₂MMT and their derived CDs including H₂PhT-CDs, H₂EMT-CDs, H₂PhMT-CDs and H₂MMT-CDs are displayed in Fig. 2. As the synthesis precursors, H₂PhT showed three characteristic absorption peaks (Fig. 2A) at 214, 311 and 345 nm, which correspond to π - π * transitions from single C=C bond, n- π * transitions of C-S and C-N bonds, and π - π * transitions of π -conjugated system composed of benzo[d]thiazole, thiourea and benzene structures, respectively. [12-14] After formation of H₂PhT-CDs, the π - π * transitions were observed at 243 nm, suggesting that H₂PhT compounds participated in CDs synthesis and the structure might be changed. H₂PhMT (Fig. 2C) displays a similar absorption spectrum to that of H₂PhT but with blue-shifted peaks. As it can be seen in Fig. 2C, the π - π * transition from π -conjugated system of H_2PhMT is at 342 nm which is slightly lower than 345 nm for H₂PhT (Fig. 2A). This difference can be explained by the fact that π-conjugated system of H₂PhMT is smaller than that of H₂PhT owing to lack of benzene ring that is coupled with thiazole. However, H₂PhMT-CDs show red-shifted π - π * transition peak at 288 nm compared to H₂PhT-CDs, indicating potentially different structures of these two CDs. Regarding H2EMT and H2MMT, two characteristic peaks were found at 255 and 290 nm ascribed to π - π * and $n-\pi$ * transitions, respectively (Fig. 2B and D). The formed H₂EMT-CDs and H₂MMT-CDs exhibit significantly different UV-vis absorption bands. In detail, H₂MMT-CDs exhibit obvious π - π * transition bands at

234 and 330 nm while H₂EMT-CDs only show a small peak at around 290 nm. Therefore, UV-vis spectra of synthesized compounds and prepared CDs may possess different optical properties.

3.2. Fluorescence spectra of H_2PhT -CDs, H_2EMT -CDs, H_2PhMT -CDs and H_2MMT -CDs

Photoluminescence (PL) is one of the most important properties of CDs that enables CDs to be used in biomedical fields, such as diagnosis, drug delivery, photodynamic therapy, and bioimaging. Meanwhile, CDs also have been involved in sensing applications. [3,15-18] Many CDs possess excitation-dependent PL emission properties. With the excitation wavelength increased, the corresponding emission wavelength usually undergoes redshifts, and the emission intensity increases first followed by a decrease. A few CDs have excitation-independent emission, which means the emission wavelengths of CDs will not be changed over the excitation wavelengths. In this study, the excitation wavelengths ranging from 350 to 400 nm with an interval of 25 nm were set to measure the PL emissions of the four as-prepared CDs. As shown in Fig. 3, with increasing the excitation wavelengths, H₂PhT-CDs (Fig. 3A), 3B) and H₂PhMT-CDs (Fig. 3C) show H₂EMT-CDs (Fig. excitation-independent PL emission at around 440 nm, while H₂MMT-CDs (Fig. 3D) exhibit excitation-dependent PL emission property.

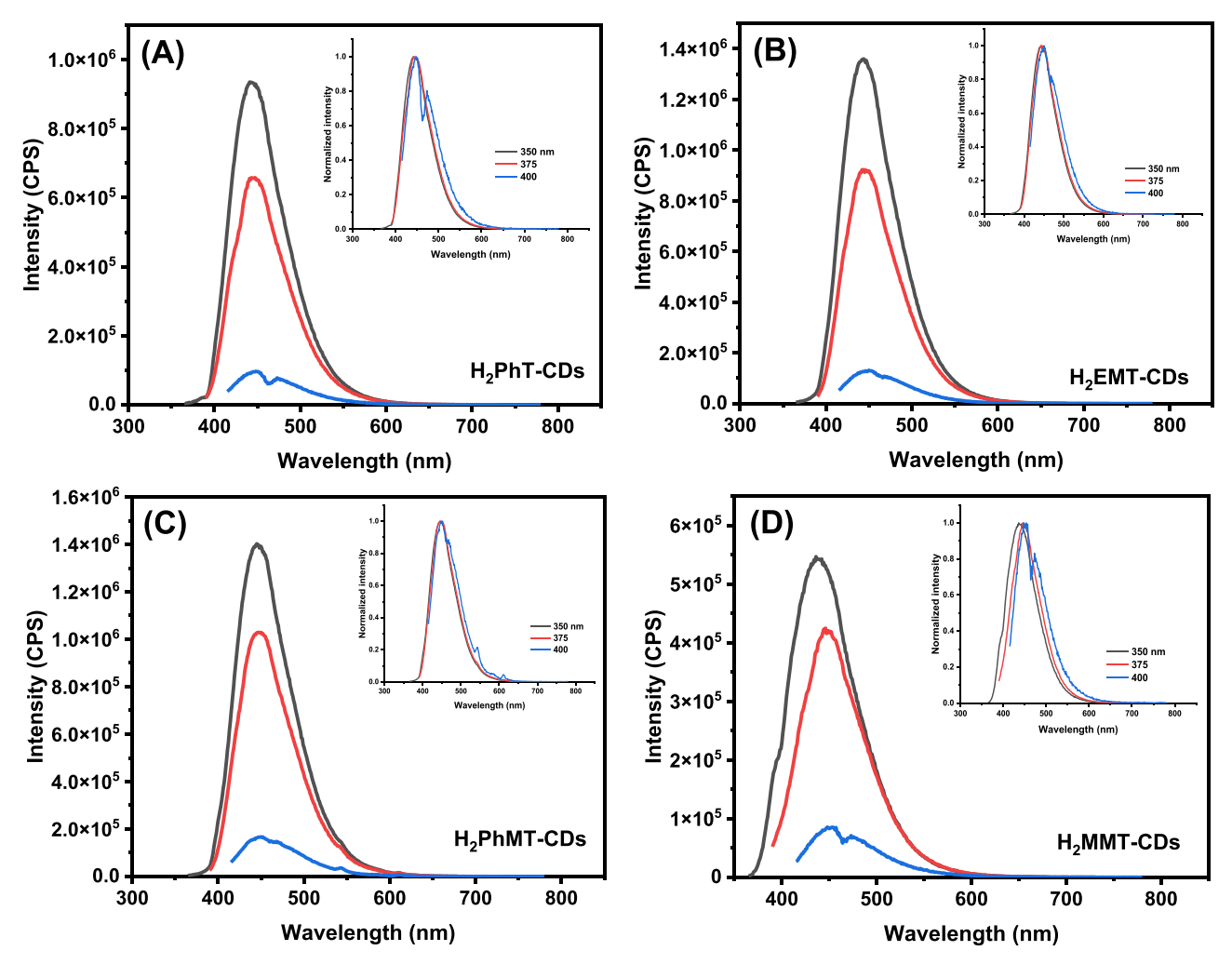


Fig. 3. Fluorescence spectra of (A) H₂PhT-CDs, (B) H₂EMT-CDs; (C) H₂PhMT-CDs; and (D) H₂MMT-CDs. The insects are the normalized fluorescence spectra.

3.3. FTIR spectra

The functional groups of precursors and CDs were measured by FTIR spectroscopy. As shown in Fig. 4 and Table 1, as one of the precursors, citric acid (CA) exhibits typical C=O stretching vibrational bands at 1744 and 1694 cm⁻¹ that are both associated to carboxyl groups. EDA shows two bands at 3360 and 3281 cm⁻¹ assigned to the asymmetric and symmetric N-H stretching vibrations from primary amines, respectively. As-prepared four compounds also display the N-H stretching vibrations bands in the range of 3177–3085 cm⁻¹ that can be ascribed to the secondary amines. The C-H stretching vibrations of these compounds were found at 2976-2922 cm⁻¹, while the C=N/C=C stretching vibrations from benzene and thiazole were observed at 1567–1523 cm⁻¹. Moreover, thiamine groups (HN-C=S), the most important moieties in medical applications, exhibit four bands in spectra at 1504–1490. 1450-1433, 1192-1187 and 837-834 cm⁻¹ which are contributed to C-N stretching, C-H bending, C=S stretching and C-S stretching vibrational modes, respectively. [5.6.11] After the solvothermal synthetic process and purifications, the CDs using above compounds as precursors were observed a wide N-H/C-H stretching absorption band ranging from 3557 to 2504 cm⁻¹ in FTIR spectrum (Fig. 4 and Table 2). Compared to precursors, H₂PhT-CDs, H₂EMT-CDs, H₂PhMT-CDs, and H₂MMT-CDs all

display a new peak at 2133 cm⁻¹ that might be corresponding to C=C=C/C=C=N stretching vibrations. Meanwhile, a new band at 1645 cm⁻¹ belonging to C=O stretching vibrations from the amide bond was also found, demonstrating that carboxyl groups of citric acid had been reacted with amine groups from EDA and one of four prepared molecules to form CDs. Then four formed CDs exhibit two characteristic bands at 1548 and 1374 cm⁻¹ that overlap with FTIR peaks related to benzene/thiazole and thiamine groups. These bands are assigned to C=N/C=C/N-H and C-H stretching vibrations, respectively. The C-N/C-O stretching vibrations of H₂PhT-CDs, H₂EMT-CDs and H₂PhMT-CDs are obviously shown at 1260 cm⁻¹. While H₂MMT-CDs show a slightly shifted C-N/C-O stretching band at 1245 cm⁻¹. In addition to these typical peaks, there are also C-S stretching vibration peaks observed in H₂PhT-CDs, H₂EMT-CDs, H₂PhMT-CDs, and H₂MMT-CDs, which appear at 894, 837, 834 and 834 cm⁻¹, respectively. Thus, FTIR spectra results suggest that H₂PhT-CDs, H₂EMT-CDs, H₂PhMT-CDs, and H₂MMT-CDs were successfully prepared in this study and that the residual structures of H₂PhT, H₂EMT, H₂PhMT and H₂MMT may still be present, which could be beneficial for medical applications in future work.

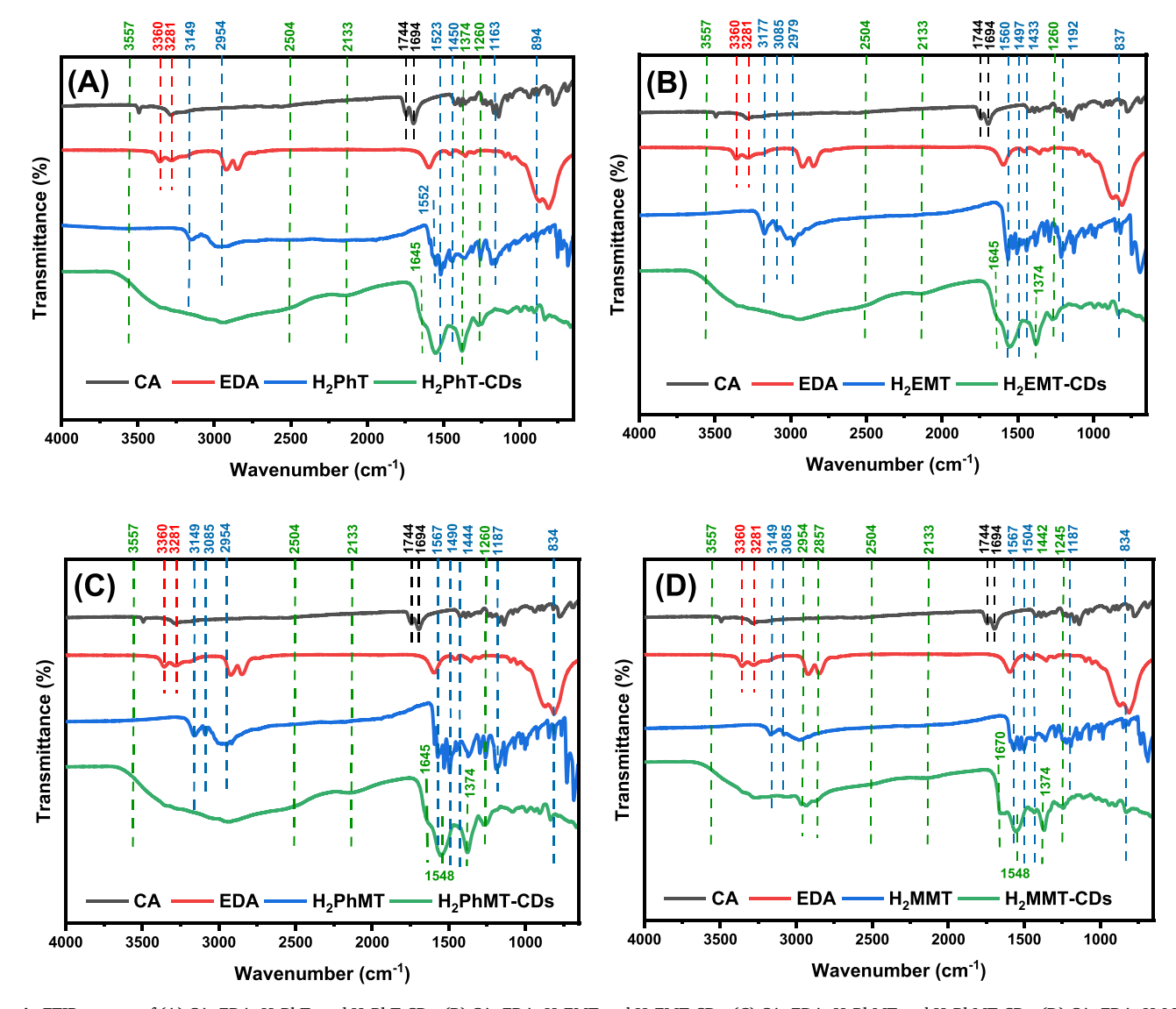


Fig. 4. FTIR spectra of (A) CA, EDA, H₂PhT, and H₂PhT-CDs, (B) CA, EDA, H₂EMT and H₂EMT-CDs; (C) CA, EDA, H₂PhMT and H₂PhMT-CDs; (D) CA, EDA, H₂MMT and H₂MMT-CDs.

Table 1 FTIR characteristic peaks of CA, EDA, H₂PhT, H₂EMT, H₂PhMT and H₂MMT.

	CA	EDA	$\rm H_2PhT$	H_2EMT	$\rm H_2PhMT$	H_2MMT
Functional groups	FTIR (cm ⁻¹)					
N-H stretching	N/A	3360, 3281	3149	3177, 3085	3149, 3085	3149, 3085
C-H stretching	3000	2922, 2848	2954	2979	2954	2954
C=C=C or C=C=N stretching	N/A	N/A	N/A	N/A	N/A	N/A
C=O stretching, carboxyl groups	1744, 1694	N/A	N/A	N/A	N/A	N/A
C=O stretching, amide bond	N/A	N/A	N/A	N/A	N/A	N/A
C=N/C=C stretching	N/A	N/A	1552, 1523	1560	1567	1567
C-N/C-O stretching	1217	1358	1260	1260	1260	1245
N-H bending	N/A	1591	1523	1560	1567	1567
C-H bending	1421	1461	1450	1497	1490	1504
thioamide group (HN-C=S)	N/A	N/A	1450, 1163, 894	1497, 1433, 1192, 837	1490, 1444, 1187, 834	1504, 1442, 1187, 834

Table 2 FTIR characteristic peaks of $H_2PhT\text{-}CDs$, $H_2EMT\text{-}CDs$, $H_2PhMT\text{-}CDs$ and $H_2MMT\text{-}CDs$.

	H ₂ PhT-CDs	H ₂ EMT- CDs	H ₂ PhMT- CDs	H ₂ MMT- CDs
Functional groups	FTIR (cm ⁻¹)	FTIR (cm ⁻¹)	FTIR (cm ⁻¹)	FTIR (cm ⁻¹)
N-H/C-H stretching	3557-2504	3557-2504	3557-2504	3557-2504
C=C=C or C=C=N stretching	2133	2133	2133	2133
C=O stretching, amide bond	1645	1645	1645	1670
C=N/C=C/N-H stretching	1548	1548	1548	1548
C-N/C-O stretching	1260	1260	1260	1245
C-H bending	1374	1374	1374	1374
C-S stretching	894	837	834	834

3.4. Thermogravimetric analysis (TGA)

Further, thermogravimetric analysis (TGA) was used to investigate the structural property of CDs. When TGA and derivative thermogravimetric analysis (DTG) were conducted on all the four CD species, four decomposition stages were generally observed, namely 40–158, 158–248, 248–463, and 463–1000 °C (Fig. 5B). According to an early study, [19] the thermal decompositions of CDs at above temperatures indicate the structures including alcoholic -OH, oxygen-containing moieties such as C-O, C—O, -COOH, amines, and graphitic cores, respectively, in different CDs. Generally, similar to other characterization results, all the four types of CDs share similar decomposition stages

and mass loss in each stage, namely (24%) 40–158, (28%) 158–248, (17%) 248–463, and (31%) 463–1000 °C, which is likely due to the same matrix composed of citric acid and excessive ethylenediamine. However, comparing the ending point in the last decomposition stage in TGA (Fig. 5A), we observed the highest temperatures to completely decompose H₂PhT-CDs and H₂EMT-CDs were similar and higher than those in H₂PhMT-CDs, and H₂MMT-CDs, which indicates a higher thermal stability of the former than the latter. It is reasonable that H₂PhT-CDs possess the highest thermal stability while H₂MMT-CDs show a lower thermal stability among the four types of CDs considering the abundance of aromatic structures brought by H₂PhT and H₂MMT. However, the rule was not followed when it came to the thermal stabilities of H₂EMT-CDs and H₂PhMT-CDs, which demonstrates the effect of matrix on the thermal stability of CDs.

3.5. AFM images

CDs are nanoparticles with a size less than 10 nm, which enable them to penetrate cell membranes and target organelles and the cellular nuclei. [20–22] In this study, the sizes of four families of CDs including $\rm H_2PhT\text{-}CDs$, $\rm H_2EMT\text{-}CDs$, $\rm H_2PhMT\text{-}CDs$, and $\rm H_2MMT\text{-}CDs$ were characterized via AFM. As shown in Fig. 6, four families of CDs are all uniformly distributed in DI water. The average diameters of $\rm H_2PhT\text{-}CDs$ (Fig. 6A), $\rm H_2EMT\text{-}CDs$ (Fig. 6B), $\rm H_2PhMT\text{-}CDs$ (Fig. 6C), and $\rm H_2MMT\text{-}CDs$ (Fig. 6D) are around 7.5, 4.2, 8.5 and 3.2 nm, respectively, inferring the successful synthesis of CDs.

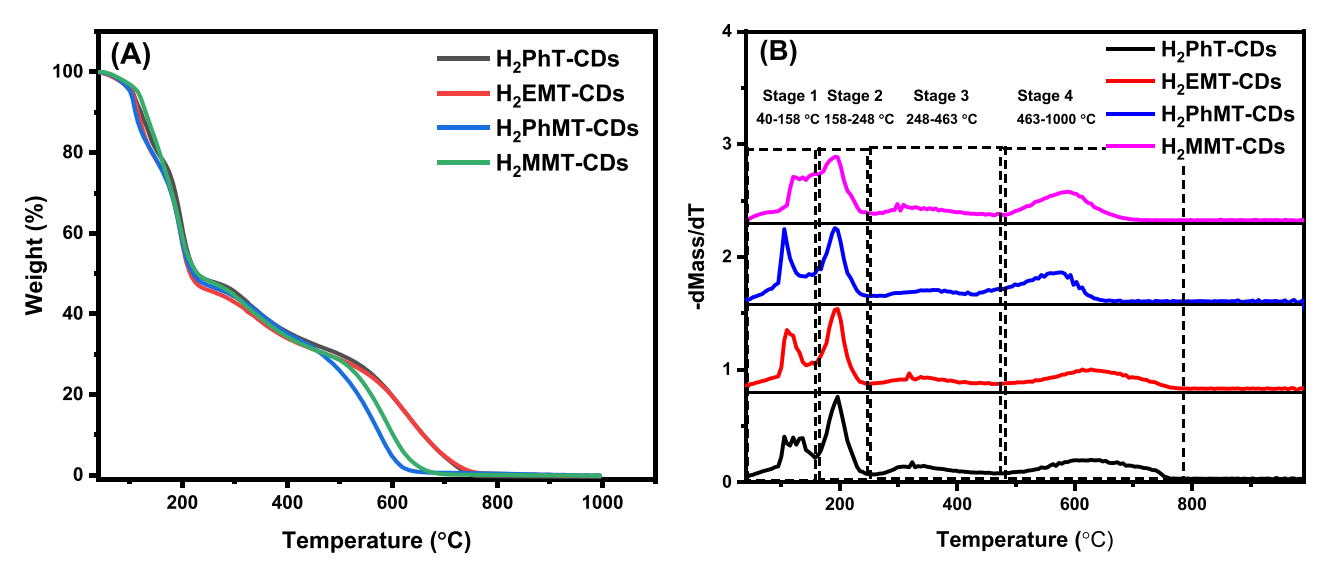


Fig. 5. TGA and DTG of H₂PhT-CDs, H₂EMT-CDs, H₂PhMT-CDs, and H₂MMT-CDs.

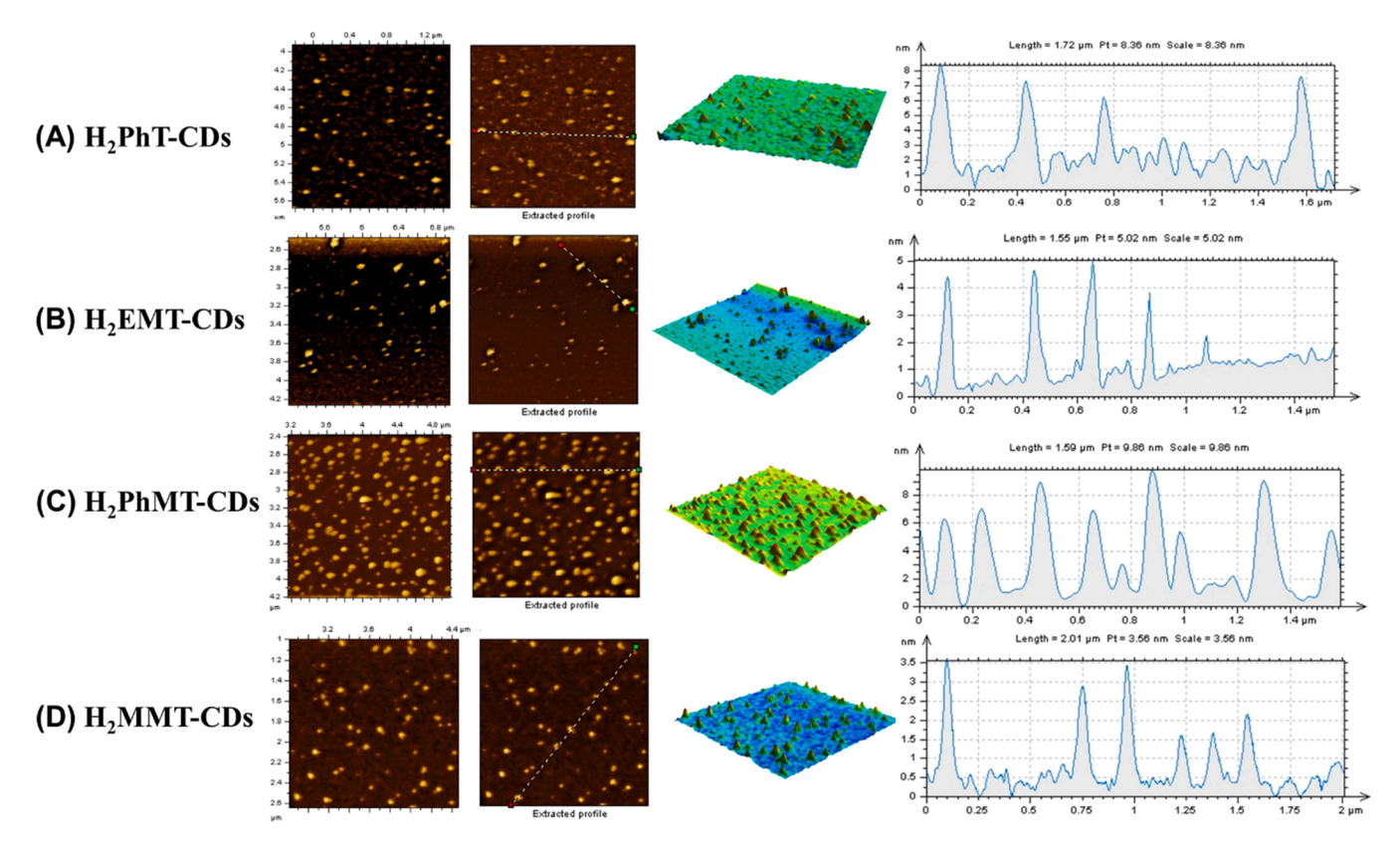


Fig. 6. AFM images of (A) H₂PhT-CDs, (B) H₂EMT-CDs; (C) H₂PhMT-CDs; and (D) H₂MMT-CDs.

3.6. Zeta potential

The surface charges of CDs play a vital role in determining the cellular uptake affinity of CDs. Previous literature has shown that nanoparticles with slightly negative, neutral, and positive charges are easier to be uptake by cells than nanomaterials with highly negative charges. [23,24] Positively charged CDs are more likely to be taken up by cells through electrostatic interactions with the negatively charged cell membrane, while negatively charged CDs may experience repulsion and lower uptake. Therefore, careful control of surface charge is important in optimizing the biological activities of CDs. To investigate whether as-prepared four families of CDs are potential candidates to enter cells with high affinity, zeta potential of H₂PhT-CDs, H₂EMT-CDs, H₂PhMT-CDs, and H₂MMT-CDs were measured in this experiment. The results are shown in Fig. 7. Based on three repeated measurements, the zeta potential of H2PhT-CDs, H2EMT-CDs, H2PhMT-CDs, and H_2MMT -CDs were calculated to be 0.710 \pm 0.610, - 3.180 \pm 2.542, -3.540 ± 2.130 and -12.100 ± 7.012 , respectively. Out of these four families of CDs, only H₂PhT-CDs display slightly positive charges, which indicate that H₂PhT-CDs might have the highest cell affinity and even show nucleus targeting ability. Such properties might lead H₂PhT-CDs to be an ideal anticancer reagent. The zeta potentials of H2EMT-CDs and H₂PhMT-CDs are both slightly negative, but less negative than that of H₂MMT-CDs. This difference might make H₂EMT-CDs and H₂PhMT-CDs a comparable cellular uptake affinity that is higher than that of H₂MMT-CDs. Since cellular uptake affinities of CDs are not solely based on surface charges but are also determined by other structural properties and sizes, the cellular uptake capabilities of these four families of CDs will be evaluated experimentally in cell lines in future work.

4. Conclusion

In summary, using molecules composed of thioureas and thiazole rings as precursors, 1-(benzo[d]thiazol-2-yl)— 3-phenylthiourea

(H₂PhT), N-ethyl-N'-(4'-methylthiazol-2'-yl) thiourea (H₂EMT), Nphenyl-N'-(4'-methylthiazol-2'-yl)thiourea (H2PhMT) and N-methyl-N'-(4'-methylthiazol-2'-yl) thiourea (H2MMT) derived CDs were successfully prepared and characterized in this project. The results show that the synthesized H₂PhT-CDs, H₂EMT-CDs, H₂PhMT-CDs, and H₂MMT-CDs with blue photoluminescence emissions possess sizes less than 10 nm. All four families of CDs were found to be slightly charged, which could promote them exhibit high cell affinity. Meanwhile, the residual structures of H₂PhT, H₂EMT, H₂PhMT and H₂MMT with potential biological applications, may still be present on the surface of CDs. Since the compounds containing thioureas and thiazole rings can be used in diabetes, antiviral, antibacterial and anticancer therapies, these four families of CDs might combine the benefit of treatment abilities of synthesized compounds and nanoparticles, showing enhanced treatment efficiency. Especially, H₂PhT-CDs with slightly positive charges might show excellent cell affinity and capability of cellular nucleus targeting, significantly improving anticancer efficiency. Overall, combination of small sizes, surface charges and surface moieties, all these four families of CDs might be potential in the treatment of diabetes, cancer, and infections in future research.

CRediT authorship contribution statement

Suhair M. S. Jambi: Conceptualization, Methodology, Validation, Formal analysis, Data curation, Investigation, Writing – review & editing, Project administration. Jiuyan Chen: Conceptualization, Methodology, Validation, Formal analysis, Data curation, Investigation, Writing – original draft, Writing – review & editing, Project administration. Wei Zhang: Methodology, Investigation, Formal analysis. Shiwei Fu: Investigation, Formal analysis, Writing – original draft. Yiqun Zhou: Formal analysis, Writing – review & editing. Justin B. Domena: Investigation, Formal analysis. Fuwu Zhang: Resources, Supervision, Validation, Writing – review & editing. Roger M. Leblanc: Conceptualization,

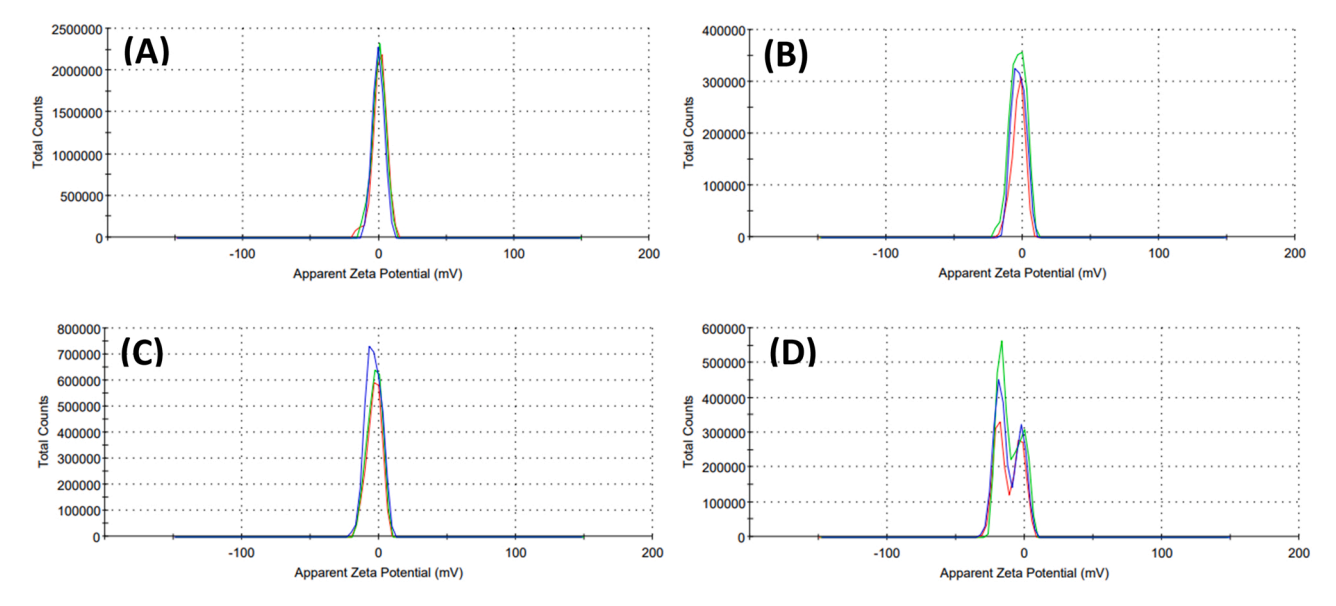


Fig. 7. Zeta potential of (A) H₂PhT-CDs, (B) H₂EMT-CDs; (C) H₂PhMT-CDs; and (D) H₂MMT-CDs.

Funding acquisition, Resources, Supervision, Visualization, Methodology, Project administration, Writing – review & editing.

Declaration of Competing Interest

The authors declare that they have no known competing financial interests or personal relationships that could have appeared to influence the work reported in this paper.

Data Availability

No data was used for the research described in the article.

Acknowledgments

Professor Roger M. Leblanc thanks the support from the National Science Foundation under grant 2041413.

Appendix A. Supporting information

Supplementary data associated with this article can be found in the online version at doi:10.1016/j.colsurfa.2023.131522.

References

- I.I. Lungu, A.M. Grumezescu, A. Volceanov, E. Andronescu, Nanobiomaterials used in cancer therapy: an up-to-date overview, Molecules 24 (19) (2019) 1–21.
- [2] H. Li, X. Yan, D. Kong, R. Jin, C. Sun, D. Du, Y. Lin, G. Lu, Recent advances in carbon dots for bioimaging applications, Nanoscale Horiz. 5 (2) (2020) 218–234.
- [3] C. Ji, Y. Zhou, R.M. Leblanc, Z. Peng, Recent developments of carbon dots in biosensing: a review, ACS Sens 5 (9) (2020) 2724–2741.
- [4] Y. Zhou, K.J. Mintz, S.K. Sharma, R.M. Leblanc, Carbon dots: Diverse preparation, application, and perspective in surface chemistry, Langmuir 35 (28) (2019) 9115–9132.
- [5] W. Zhang, J. Chen, J. Gu, M. Bartoli, J.B. Domena, Y. Zhou, B.C.L.B. Ferreira, E. K. Cilingir, C.M. McGee, R. Sampson, C. Arduino, A. Tagliaferro, R.M. Leblanc, Nano-carrier for gene delivery and bioimaging based on pentaetheylenehexamine modified carbon dots, J. Colloid Interface Sci. 639 (2023) 180–192.
- [6] J. Chen, F. Li, J. Gu, X. Zhang, M. Bartoli, J.B. Domena, Y. Zhou, W. Zhang, V. Paulino, B.C.L.B. Ferreira, N. Michael Brejcha, L. Luo, C. Arduino, F. Verde, F. Zhang, F. Zhang, A. Tagliaferro, J.H. Olivier, Y. Zhang, R.M. Leblanc, Cancer cells inhibition by cationic carbon dots targeting the cellular nucleus, J. Colloid Interface Sci. 637 (2023) 193–206.
- [7] L.-N. Wu, Y.-J. Yang, L.-X. Huang, Y. Zhong, Y. Chen, Y.-R. Gao, L.-Q. Lin, Y. Lei, A.-L. Liu, Levofloxacin-based carbon dots to enhance antibacterial activities and combat antibiotic resistance, Carbon 186 (2022) 452–464.

- [8] S. Lu, L. Liu, H. Wang, W. Zhao, Z. Li, Z. Qu, J. Li, T. Sun, T. Wang, G. Sui, Synthesis of dual functional gallic-acid-based carbon dots for bioimaging and antitumor therapy, Biomater. Sci. 7 (8) (2019) 3258–3265.
- [9] S. Huang, J. Gu, J. Ye, B. Fang, S. Wan, C. Wang, U. Ashraf, Q. Li, X. Wang, L. Shao, Y. Song, X. Zheng, F. Cao, S. Cao, Benzoxazine monomer derived carbon dots as a broad-spectrum agent to block viral infectivity, J. Colloid Interface Sci. 542 (2019) 198–206.
- [10] M.S. Jambi, Quantum, characterization and spectroscopic studies on Cu(II), Pd(II) and Pt(II) complexes of 1-(benzo[d]thiazol-2-yl)-3-phenylthiourea and its biological application as antimicrobial and antioxidant, J. Mol. Struct. 1143 (2017) 217–228.
- [11] S.M.S. Jambi, Cd(II), Hg(II) and Pt(II) complexes of 1-ethyl-3-(4-methylthiazol-2-yl)thiourea: Synthesis, X-ray crystal structure, DFT studies, antimicrobial and antioxidant applications, J. Mol. Liq. 262 (2018) 237–247.
- [12] E. İnkaya, Synthesis, X-ray structure, FT-IR NMR (13C/1H), UV-vis spectroscopy, TG/DTA study and DFT calculations on 2-(benzo[d]thiazol-2-ylthio)-1-((1s, 3s)-3-mesityl-3-methylcyclobutyl) ethan-1-one, J. Mol. Struct. 1173 (2018) 148–156.
- [13] A. Saeed, P.A. Channar, G. Shabir, F.A. Larik, Green synthesis, characterization and electrochemical behavior of new thiazole based coumarinyl scaffolds, J. Fluoresc. 26 (3) (2016) 1067–1076.
- [14] M. Sivadhayanithy, L. Ravikumar, C. Rengaswamy, Design and synthesis of new thermally stable polyesters containing azo and phenylthiourea groups, High. Perform. Polym. 19 (1) (2006) 62–77.
- [15] Y. Zhou, J. Chen, E. Kirbas Cilingir, W. Zhang, L. Gonzalez, S. Perez, A. Davila, N. Brejcha, J. Gu, W. Shi, J.B. Domena, B. Ferreira, F. Zhang, F.A. Vallejo, D. Toledo, P.Y. Liyanage, R.M. Graham, J. Dallman, Z. Peng, C. Agatemor, A. Catenazzi, R.M. Leblanc, An insight into embryogenesis interruption by carbon nitride dots: can they be nucleobase analogs? Nanoscale 14 (47) (2022) 17607–17624.
- [16] G. Nocito, G. Calabrese, S. Forte, S. Petralia, C. Puglisi, M. Campolo, E. Esposito, S. Conoci, Carbon dots as promising tools for cancer diagnosis and therapy, Cancers (Basel) 13 (9) (2021) 1–14.
- [17] N. Xu, J. Du, Q. Yao, H. Ge, H. Li, F. Xu, F. Gao, L. Xian, J. Fan, X. Peng, Precise photodynamic therapy: Penetrating the nuclear envelope with photosensitive carbon dots, Carbon 159 (2020) 74–82.
- [18] P. Das, M. Bose, S. Ganguly, S. Mondal, A.K. Das, S. Banerjee, N.C. Das, Green approach to photoluminescent carbon dots for imaging of gram-negative bacteria Escherichia coli, Nanotechnology 28 (19) (2017) 1–12, 195501.
- [19] Y. Zhou, N. Kandel, M. Bartoli, L.F. Serafim, A.E. ElMetwally, S.M. Falkenberg, X. E. Paredes, C.J. Nelson, N. Smith, E. Padovano, W. Zhang, K.J. Mintz, B.C.L. B. Ferreira, E.K. Cilingir, J. Chen, S.K. Shah, R. Prabhakar, A. Tagliaferro, C. Wang, R.M. Leblanc, Structure-activity relationship of carbon nitride dots in inhibiting Tau aggregation, Carbon 193 (2022) 1–16.
- [20] B. Unnikrishnan, R.S. Wu, S.C. Wei, C.C. Huang, H.T. Chang, Fluorescent carbon dots for selective labeling of subcellular organelles, ACS Omega 5 (20) (2020) 11248–11261.
- [21] P. Gao, S. Liu, Y. Su, M. Zheng, Z. Xie, Fluorine-doped carbon dots with intrinsic nucleus-targeting ability for drug and dye delivery, Bioconjug Chem. 31 (3) (2020) 646–655.

- [22] W. Su, R. Guo, F. Yuan, Y. Li, X. Li, Y. Zhang, S. Zhou, L. Fan, Red-emissive carbon quantum dots for nuclear drug delivery in cancer stem cells, J. Phys. Chem. Lett. 11 (4) (2020) 1357–1363.
- [23] G.-Y. Lee, P.-Y. Lo, E.-C. Cho, J.-H. Zheng, M. Li, J.-H. Huang, K.-C. Lee, Integration of PEG and PEI with graphene quantum dots to fabricate pH-responsive nanostars for colon cancer suppression in vitro and in vivo, FlatChem 31 (2022) 1–7.
- [24] Z. Zhu, Q. Li, P. Li, X. Xun, L. Zheng, D. Ning, M. Su, Surface charge controlled nucleoli selective staining with nanoscale carbon dots, PLoS One 14 (5) (2019) 1–11, e0216230.